J. Astrophys. Astr. (1983) **4**, 135-149

Nonlinear Development of Convective Instability within Slender Flux Tubes. I. Adiabatic Flow

P. Venkatakrishnan *Indian Institute of Astrophysics, Bangalore 560034*

Received 1983 February 23; accepted 1983 June 15

Abstract. The nonlinear development of convective instability within slender flux tubes is studied using the method of characteristics. It is seen that the initial magnetic field influences the development of the instability. The asymptotic state of the unstable tube depends on the boundary conditions. Flux tubes subjected to 'open' boundary conditions show a better evidence for field amplification than those subjected to 'closed' boundary conditions. In either case, convective instability results in the generation of significant gas flow within slender flux tubes.

Key words: Sun, magnetic field – Sun, convection – fluid dynamics, unsteady flow

1. Introduction

The concentration of photospheric magnetic field into intense flux tubes can occur either due to the interaction of convection with an initially distributed magnetic flux, or due to a convective instability of a hydrostatic flux tube. A preliminary calculation by Parker (1963) based on the first scenario yielded unlimited field amplification in regions where convective flow converged into downdrafts. Numerical studies of this process by Weiss (1966) showed expulsion of field from centres of two-dimensional cells and concentration of field at their boundaries. This calculation ignored the dynamical reaction of field on the flow. Inclusion of dynamical effects along with an energy equation in a Boussinesq fluid by Galloway & Moore (1979) yielded a maximum value of the concentrated field which was a few times the 'equipartion field' given by $B_e \simeq (4\pi\varrho)^{\frac{1}{2}} U$ where ϱ and U are some representative values of the density and velocity of the fluid respectively. All these calculations do not satisfactorily explain the kilogauss fields seen in the photosphere. Moreover, the asymptotic configurations arising from the interaction of magnetic field with convection preclude motions within the intense magnetic sructures. This is contrary to observational results (*e.g.* Beckers & Schröter 1968; Giovanelli & Ramsay 1971; Sheeley 1971; Simon & Zirker 1974; Harvey & Hall 1975; Giovanelli & Slaughter 1978).

The second alternative of convective instability within flux tubes seems to be a natural consequence of the first process. The moderately intense fields of a few hundred gauss which result from magneto-convection are prone to a convective instability if the intensity is smaller than a critical value (Webb & Roberts 1978). A detailed numerical study of the linear stability of slender flux tubes in a realistic atmosphere (Spruit & Zweibel 1979) showed this critical value to be ~ 1300 G for the fundamental mode and larger for higher harmonics. These critical values depend on the boundary conditions used (*cf.* Unno & Ando 1979). If the instability sets in as a downward flow, the tube is expected to collapse to a higher field intensity (Parker 1978). The resulting enhancement of field was expected to quench the instability. Spruit (1979) calculated the new equilibrium states corresponding to some initial unstable equilibrium and he obtained a concentrated field of 1800 G at $\tau_{5000} = 1.0$ from an 'equipartition' field of 700 G.

Several questions have to be answered before one fully understands this process. The first question is whether the magnetic field does inhibit convective instability when nonlinearities are taken into account. The second is whether the final state of the unstable tube depends so crucially on the direction of initial flow as has been made out in the literature. A third question is about the dynamical status of the final state, *viz.* whether one ends up with a hydrostatic or a hydrodynamic flux tube. These questions can be answered only by studying the time-dependent evolution of the instability to large amplitudes from an initial unstable state. Hasan (1982) performed such a calculation for a tube with realistic initial stratification. However, his results do not include the case of small initial magnetic field. The present paper attempts to study the instability of a shorter tube with an initial polytropic stratification. The consequent gain of economy in computer time has been utilised in extending the calculations to larger durations and for more numbers of parameters. In Section 2, the basic equations along with the assumed initial and boundary conditions are described as well as the method of their solution. In Section 3 the results are described and discussed. A summary of the results is provided in Section 4.

2. Theory

2.1 *Basic Equations*

The advantage of using the slender flux tube (SFT) approximation is that arbitrary stratification of the gas along the tube can be considered without increasing the dimensions of the system of equations. One only checks whether the approximation remains valid at every epoch of the calculation. The SFT approximation is valid as long as the longitudinal variation of the tube diameter has a length-scale which is larger than the diameter. The nonlinear adiabatic equations of a SFT have been rigorously derived by Roberts & Webb (1978). They are:

$$\frac{\partial}{\partial t}(\varrho/B) + \frac{\partial}{\partial z}(\varrho v/B) = 0, \tag{2.1.1}$$

$$\varrho\frac{\partial}{\partial t}v + \varrho v\frac{\partial}{\partial z}v + \frac{\partial}{\partial z}p + \varrho g = 0, \tag{2.1.2}$$

$$\left(\frac{\partial}{\partial t}p + v\frac{\partial}{\partial z}p\right) - \frac{\gamma p}{\varrho}\left(\frac{\partial}{\partial t}\varrho + v\frac{\partial}{\partial z}\varrho\right) = 0, \tag{2.1.3}$$

$$p+\frac{B^2}{8\pi}-p_e=0, \tag{2.1.4}$$

where ϱ, v, B and p are the density, velocity, magnetic field intensity and gas pressure inside the tube while p_e is the gas pressure outside the tube. The adiabatic condition (2.1.3) is strictly valid only when the radiative diffusion time-scale is significantly larger than the sound travel time (Webb & Roberts 1980). For optically thick disturbances of radiative diffusivity $\varkappa$ this condition reduces to $\varkappa \ll g^{\frac{1}{2}} \Lambda^{\frac{3}{2}}$ where g is the acceleration due to gravity and Λ is the pressure scale-height. For Spruit's (1977) model this condition is sastified at depths of a few hundred kilometres below the photosphere. Equations (2.1.1)– (2.1.4) form a system of hyperbolic partial differential equations (in t and z) and possess three real characteristics. The slopes of these characteristics in the $t-z$ plane are given by

$$\lambda_\pm = \left(\frac{dt}{dz}\right)_\pm = \frac{1}{(v \pm C_T)}, \tag{2.1.5}$$

$$\lambda_0 = \left(\frac{dt}{dz}\right)_0 = \frac{1}{v}, \tag{2.1.6}$$

and

$$C_T = \frac{SA}{(S^2+A^2)^{\frac{1}{2}}}, \tag{2.1.7}$$

where $S=(\gamma p/\varrho)^{\frac{1}{2}}$ is the sound speed, $A=B/(4\pi\varrho)^{\frac{1}{2}}$ is the Alfven speed and C_T is the speed of tube waves. The compatibility equations along these characteristics are

$$dp_\pm \pm \varrho C_T dv_\pm = -(\varrho_e g v C_T^2/A^2 \pm \varrho C_T g)dt \quad \text{along } \lambda_\pm \tag{2.1.8}$$

and

$$dp_0 - S^2 d\varrho_0 = 0 \quad \text{along } \lambda_0 \tag{2.1.9}$$

2.2 *Initial Conditions*

The configuration of the tube at $t=0$ was chosen to be a polytrope with equal temperatures inside and outside the tube. In this case the magnetic field also varies with a scale-height that is twice that of the pressure scale-height. The ratio of the gas pressure to the magnetic pressure is thus a constant denoted by β. The initial values are given by

$$T = T_b - \frac{\Gamma-1}{\Gamma}(g/R)z, \tag{2.2.1}$$

$$\varrho = \varrho_b (T/T_b)^{1/(\Gamma-1)}, \tag{2.2.2}$$

$$p = p_b (\varrho/\varrho_b)^{\Gamma}, \tag{2.2.3}$$

$$B = (8\pi p/\beta)^{\frac{1}{2}}, \tag{2.2.4}$$

where Γ is the polytropic index, g is the acceleration due to gravity, $\mathscr{R}$ is the universal gas constant and subscript 'b', represents the value at the base of the tube. All variables were expressed in dimensionless form in terms of the following reference quantities:

velocity V_*	$= (\mathscr{R}T_b)^{\frac{1}{2}}$	pressure $p_* = \varrho_b V_*^2$	
length L_*	$= \mathscr{R}T_b/g$	magnetic field B_*	$= (8\pi p_*)^{\frac{1}{2}}$
time τ_*	$= L_*/V_*$	temperature T_*	$= T_b$
density ϱ_*	$= \varrho_b V_*^2$		

The time-dependent equations (2.1.1)–(2.1.4) were also recast in dimensionless form in a similar fashion. The initial velocity perturbation was prescribed in the form of a half sine-wave with nodes at either end of the tube. The amplitude of the perturbation (which would be either positive or negative) is yet another parameter of the problem. In the present calculations, the amplitude was chosen to be 1 per cent of the reference velocity V_*.

2.3 *Boundary Conditions*

Two alternative sets of boundary conditions were applied at the top and bottom of the tube. In one set, the gas pressure at the bottom was kept invariant in time. Since the external gas pressure was considered to be time-independent, the horizontal pressure balance, as expressed by Equation (2.1.4), implied that the local field intensity was constant in time. This meant that the foot of the flux tube was constrained to maintain a constant area of cross-section. Such a constraint might really exist at a depth of a thousand kilometres below the solar photosphere. The present calculation merely attempt to simulate such an effect, since the total length of the tube considered here equals only one scale-height in terms of the reference temperature T_b. In the first case, a similar constraint was applied to the top of the tube. Such a constraint may not exist for vertical tubes in the Sun, since this requires strong enough external flows to confine the tube. However, for tubes that bend back to the photosphere at low heights, the expansion of the tube walls implies pushing up the overlying atmosphere. Similarily contraction of the tube implies pulling up the underlying atmosphere (below the horizontal portion of the tube). This may not be easily possible and hence the constant pressure boundary condition may be appropriate for such tubes. For brevity we will call this boundary condition as the 'closed-closed boundary condition' and the tubes where this is applied as 'closed' tubes.

In the other set of calculations, the same boundary condition at the bottom of the tube was retained. The pressure at the top was however allowed to vary in such a manner as to make the Lagrangian time derivative of the pressure vanish. Such a condition implies that gas does not escape horizontally from the top of the tube, but moves up or down as to maintain constant Lagrangian pressure. This boundary condition will be referred to as 'closed-open boundary condition' and the tubes constrained by this condition was assumed so as to simulate the behaviour of open flux tubes.

2.4 *Method of Solution*

Equations (2.1.8) and (2.1.9) were integrated in time using a backward marching

scheme by the method of characteristics. In this method, the characteristics were drawn back to some earlier time-line and the values of the variables at the points of intersection of the characteristics with the earlier time-line were used to predict the values at the origin of these characteristics (for details, see Zucrow & Hoffman 1976). Since the scheme was an explicit one, the time-step was chosen to be small enough to satisfy the Courant-Friedrichs-Lewy stability condition. The spatial step-length was chosen to be 0.02 times the total length of the tube which gave an accuracy of ~ 0.0004. Starting from the initial time $t = 0$, the equations were integrated for large times of ~ 40 dimensionless time-units, which corresponded to 40 free-fall time-scales.

3. Results and discussion

The more interesting aspect of the present study can be seen in the time profiles of the various fluid dynamical variables. The spatial profile at any given instant can at best provide only a check on the SFT approximation. At $t = 0$, the radius at the top of the tube was taken as $\simeq (B_0/B_e)^{\frac{1}{2}} R_0$ where B_0 and B_e are the observed and equipartition fields respectively while R_0 is the observed radius of the collapsed tube. For $B_e \simeq 700$ G and $B_0 \simeq 1400$ G, $R_0 \sim 100$ km, the initial tube radius is $\simeq 170$ km. For $T_b = 10^4$K, the intial scale-length for variation of tube radius is $\simeq 700$ km at the top of the tube. Thus the SFT approximation is satisfactory at the top and quite good at greater depths. However, for $t > 0$, the behaviour subsequent to the development of large curvature in the tube should be viewed with a certain amount of scepticism since the SFT approximation becomes invalid. However, the spatial profiles become of great interest in cases where asymptotic steady states are attained as they can be used to predict the class of steady state solutions that are physically relevant.

The variation of velocity with time will be given more emphasis in what follows purely because of the high sensitivity of this quantity to changes in external parameters. The general behaviour can be broadly divided into three phases. The intial phase consists of a linear increase in velocity with time until the velocity attains a value which is approximately *e*-times the initial perturbation. This phase will be referred to in what follows as the linear phase. The approach to the *e*-folded velocity is generally oscillatory with a period of one tube travel time (time taken for tube waves to travel over the length of the tube). This is illustrated in Fig. 1, which shows the variation of velocity (at $z = 0.5880$) with time for $\Gamma = 3.0$, $\gamma = 1.95$ and for different values of β. These calculations were for the closed tube. Two facts can be noticed in this curve. First, the times of onset of rapid instability (as seen from a change in the slope of velocity-versus-time curves) increase with decreasing value of β. Thus larger initial magnetic fields inhibit the onset of rapid instability for a longer duration of time. Second, the approach to the phase of rapid variation is more oscillatory for larger initial fields. These oscillations arise purely because of the initial perturbations at $t = 0$. Since we are considering an adiabatic inviscid fluid, one would expect the oscillations to persist for all $t > 0$, unless the mean state changes on a time scale which is shorter than the oscillation period.

Fig. 2 shows the further development of the instability in the nonlinear phase. This phase itself consists of an initial rapid increase of the downflow followed by a less rapid increase. The most violent phase of the instability lasts only for a few free-fall time-scales. For the cases $\beta = 7.5$ and $\beta = 10.0$, the nonlinear phase could not be calculated since at earlier epochs, the transient pressure enhancement at the bottom of the tube made the gas pressure inside the tube exceed the external gas pressure. This

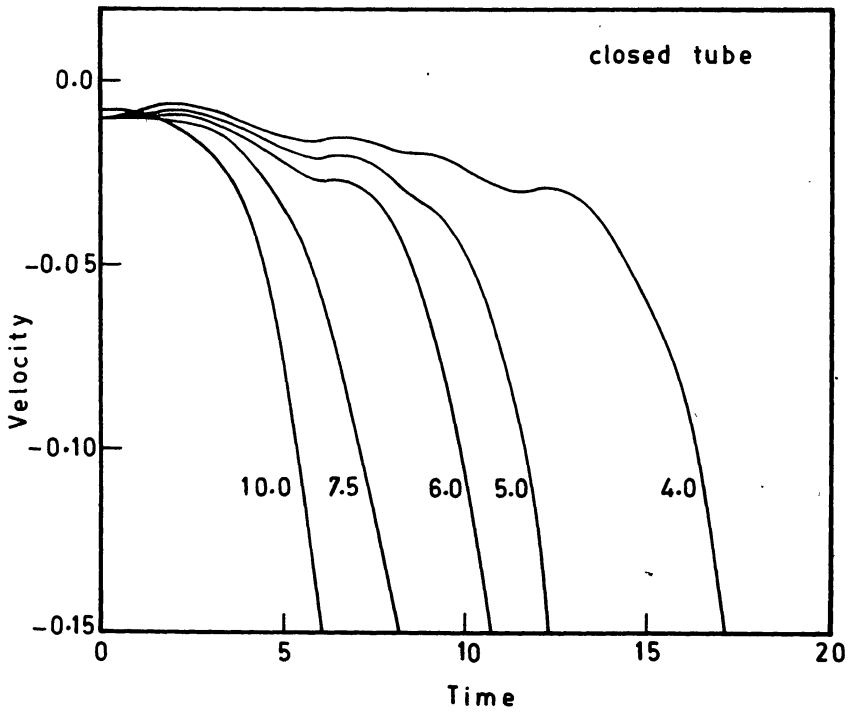

Figure 1. Variation of velocity with time at $z = 0.5880$ in the linear phase for $\Gamma = 3.0$, $\gamma = 1.95$ and $\beta = 10.0$, 7.5, 6.0, 5.0 and 4.0. Closed-closed boundary conditions are used.

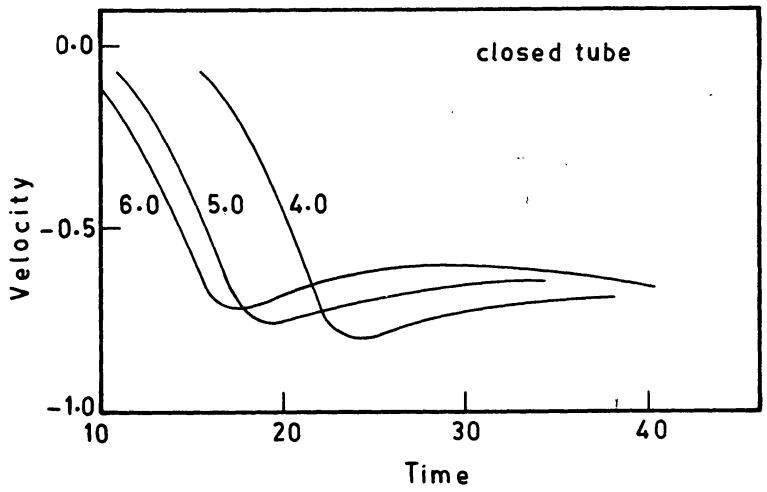

Figure 2. Variation of velocity with time for a closed tube at $z = 0.5880$ in the nonlinear phase for $\Gamma = 3.0$, $\gamma = 1.95$ and $\beta = 6.0$, 5.0 and 4.0.

meant imaginary field in the SFT approximation. In a realistic situation, either the local dilatation of the tube would set up restoring tension forces, or the transient pressure enhancement would propagate as a pressure pulse in a horizontal direction out-

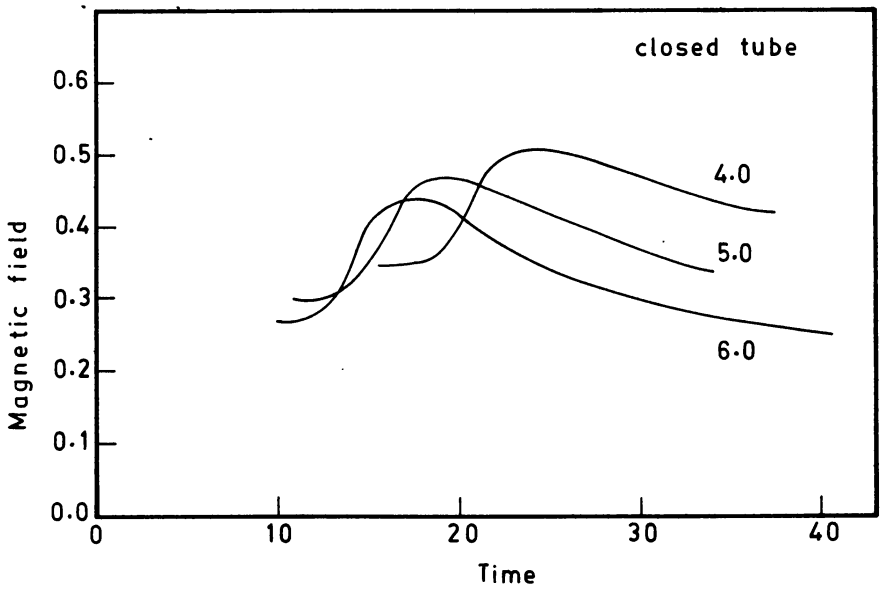

Figure 3. Time profile of nonlinear changes in magnetic field of a closed tube at $z = 0.5880$ for $\Gamma = 3.0$, $\gamma = 1.95$ and $\beta = 6.0$, 5.0 and 4.0.

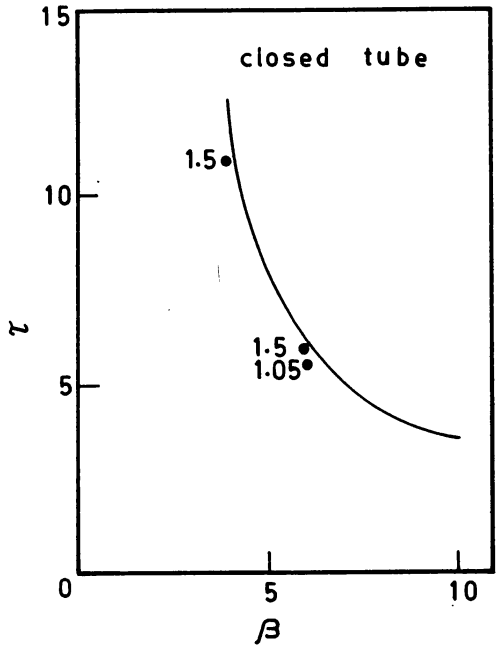

Figure 4. The time τ of onset of violent phase of instability is plotted against β for a closed tube with $\Gamma = 3.0$. The curve represents the values for $\gamma = 1.95$, while the values for different γ are plotted as filled circles.

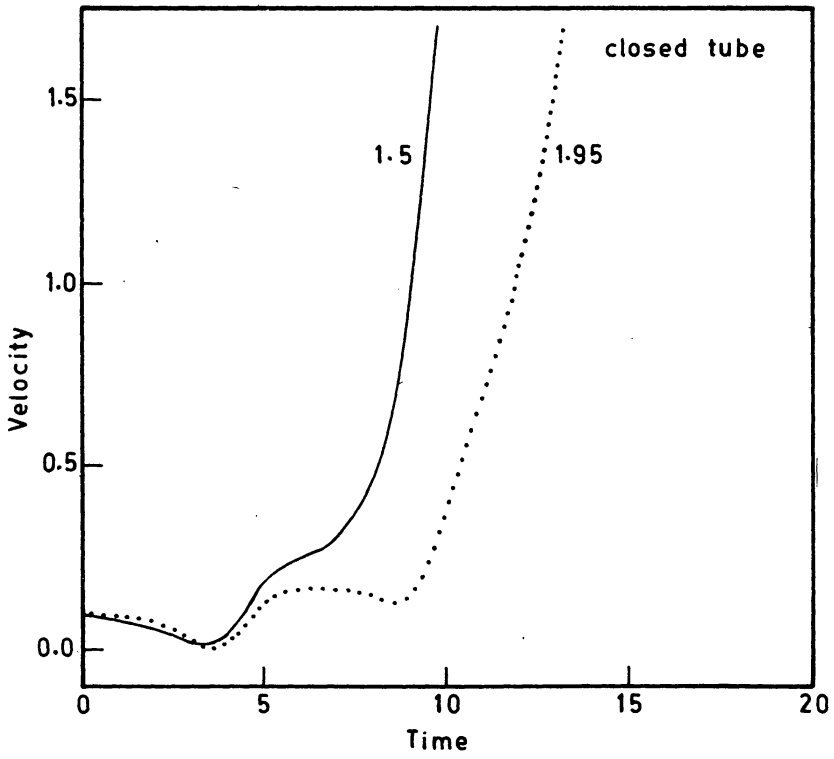

Figure 5. Response of the tube to initial upflow is depicted for small-amplitude domain. The filled and dotted lines represent the variation of tubes with $\gamma = 1.95$ and $\gamma = 1.50$ respectively. $\Gamma = 3.0$ and $\beta = 6.0$ in both the cases.

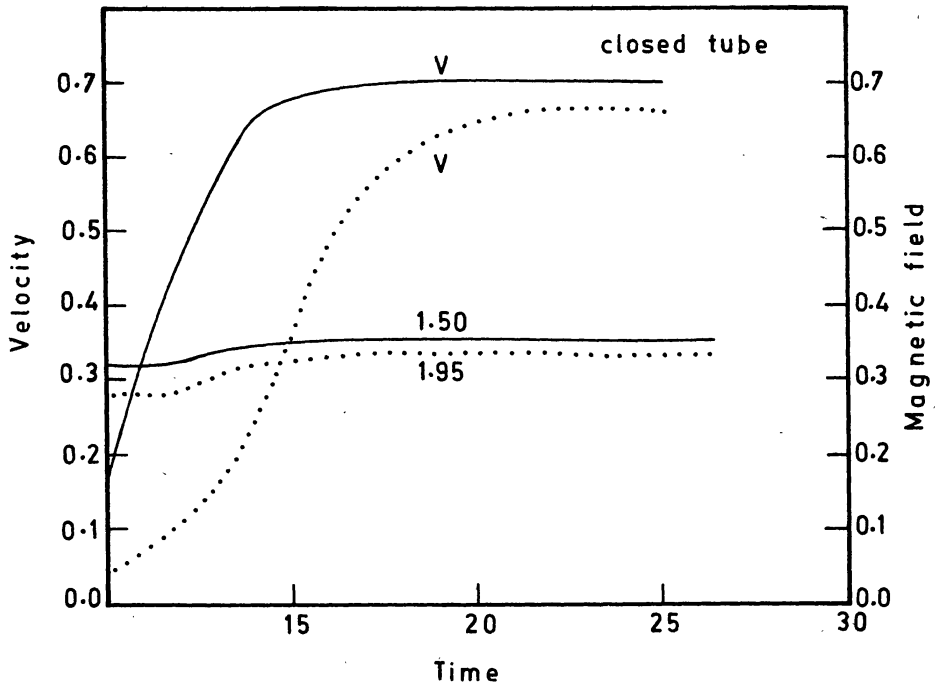

Figure 6. Large amplitude changes in velocity (marked with a V) and magnetic field of a closed tube are plotted as a function of time for parameters that are the same as in Fig. 5.

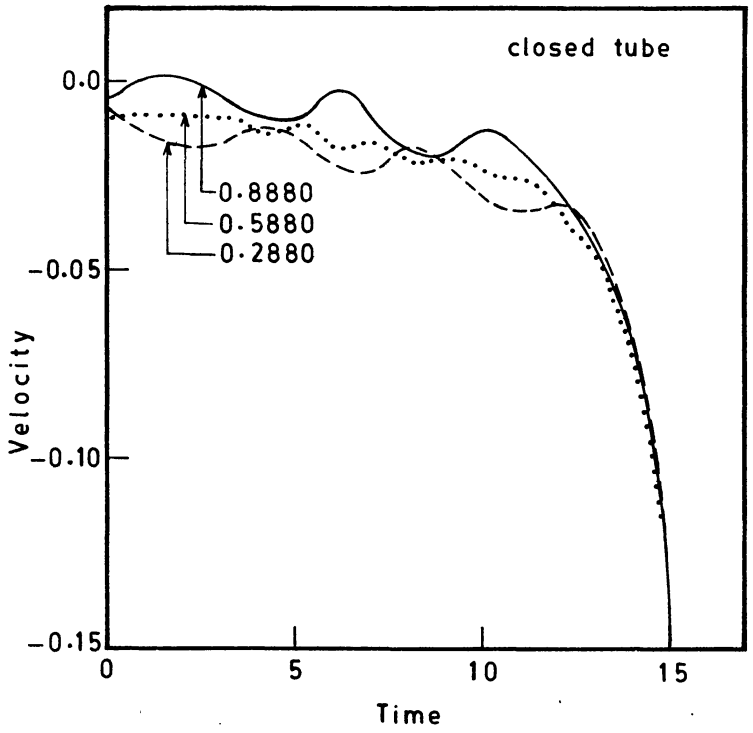

Figure 7. Linear phase of instability of a closed tube with $\Gamma = 3.0$, $\gamma = 1.5$ and $\beta = 4.0$. The velocity is plotted for three values of $z = 0.2880$ (dashed line), 0.5880 (dotted line) and 0.8880 (solid line) respectively.

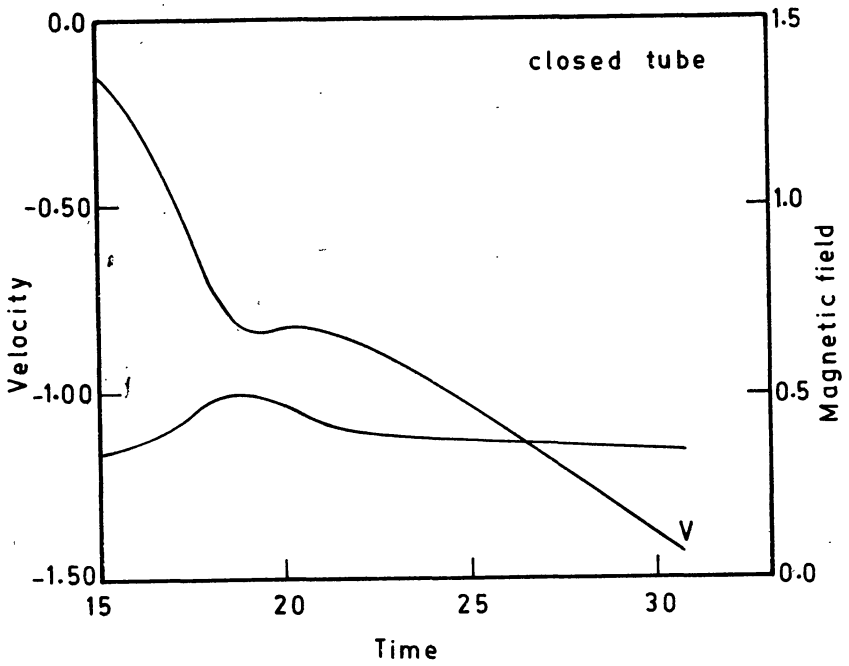

Figure 8. Nonlinear behaviour of an unstable closed tube with $\Gamma = 3.0$, $\gamma = 1.5$, and $\beta = 4.0$. Profiles of both the velocity (marked with a V) and magnetic field are shown for $z = 0.5880$.

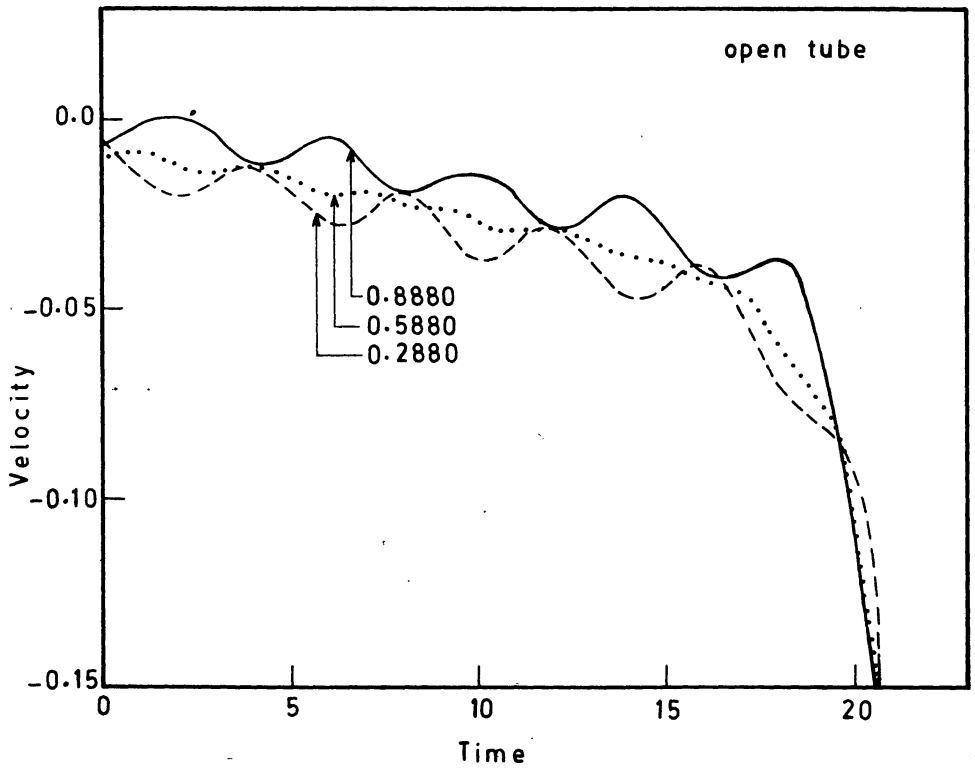

Figure 9. The variation of velocity with time is plotted for an open tube with $\Gamma = 3.0$, $\gamma = 1.95$, and $\beta = 4.0$ at three values of $z = 0.8880$ (solid line), 0.5880 (dotted line) and 0.2880 (dashed line) respectively. Only the linear phase is shown here.

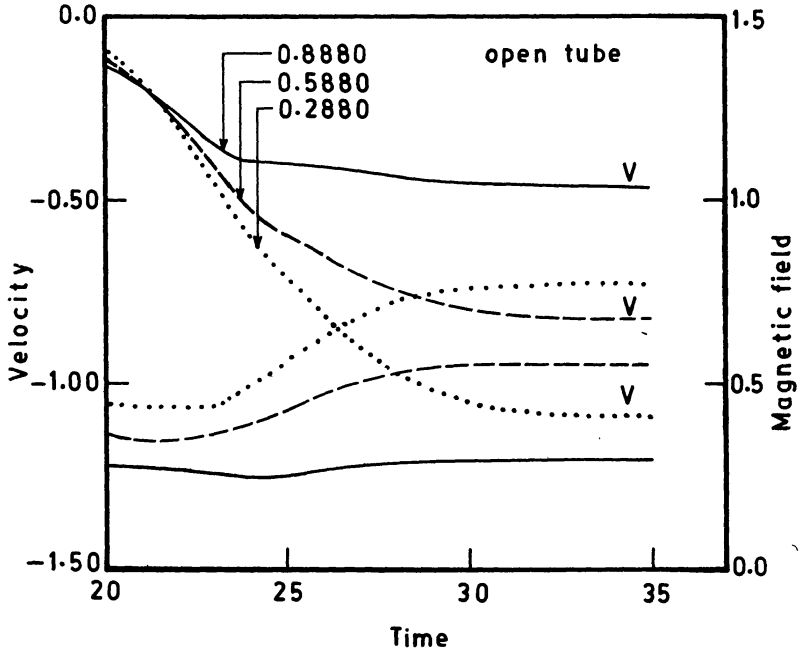

Figure 10. Large time-behaviour of an open tube with $\Gamma = 3.0$, $\gamma = 1.95$ and $\beta = 4.0$. Profiles of both velocity (marked with a V) and magnetic field are shown for three values of $z = 0.8880$ (solid line), 0.5880 (dashed line) and 0.2880 (dotted line) respectively.

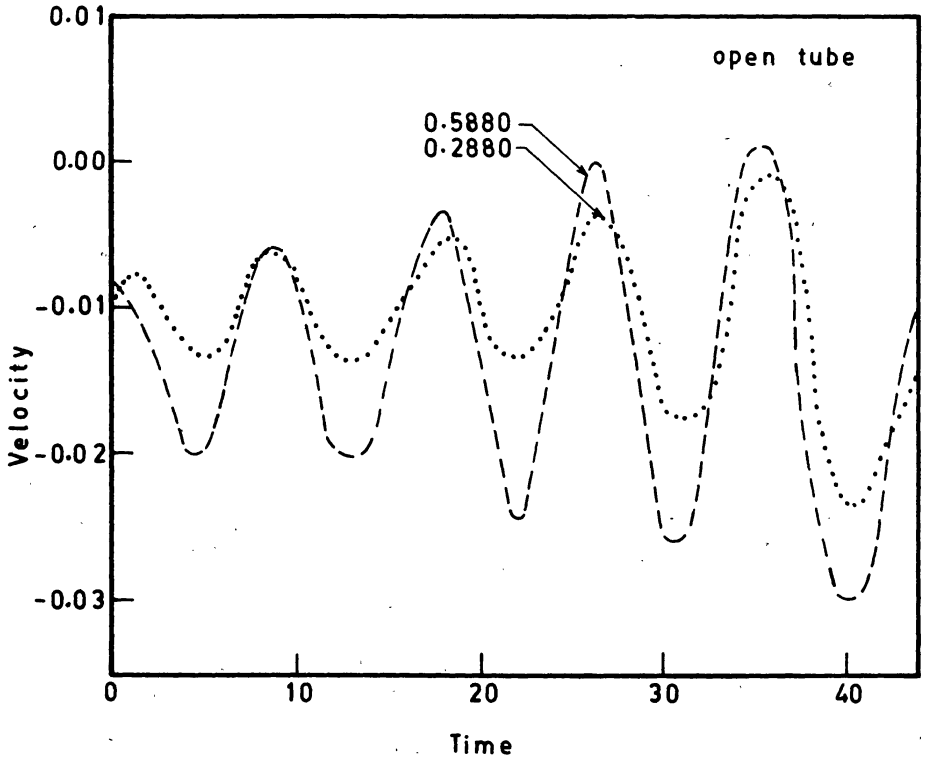

Figure 11. Change of velocity with time is shown for an open tube with $\Gamma = 3.0$, $\beta = 2.0$, $\gamma = 1.95$, and $z = 0.5880$ (dashed line) and 0.2880 (dotted line) respectively.

side the tube. For smaller β no steady state was achieved even after several tens of free-fall time-scales. Fig. 3, which shows the behaviour of the magnetic field, does not indicate any long-lasting intensification of the field. What we do see is an initial increase of magnetic field followed by a decrease (in the case of $\beta = 6.0$ even to a value smaller than the initial field). What we do not know is whether this is part of a general long-period oscillatory behaviour. The amplitude of the transient field intensification did not seem to change drastically with β.

Fig. 4 shows the stabilising influence of the magnetic field. The time τ of onset of violent instability is plotted against β. It is seen that the curve changes slope and moves towards large values of τ for small values of β. For comparison, τ for different values of γ are also marked in the same figure. As expected, the decrease of γ (increase of super-adiabaticity) causes a decrease of τ which indicates greater instability.

In order to see the effect of change in the direction of perturbation, calculations were also performed for initial upflow. Fig. 5 shows the linear regime for $\beta = 6.0$ and two values of γ (1.5 and 1.95). Here too, the onset of rapid phase is earlier for the smaller values of γ. Fig. 6 shows the nonlinear behaviour. In this case we see that a steady state with intensified field is attained, but with an upflow.

Figs 7 and 8 show the time behaviour of velocity and magnetic field for $\gamma = 1.5$ and $\beta = 4.0$. The instability is more pronounced as compared with the case for $\beta = 4.0$ and $\gamma = 1.95$. The nonlinear regime shows a continued increase of downflow and gradual

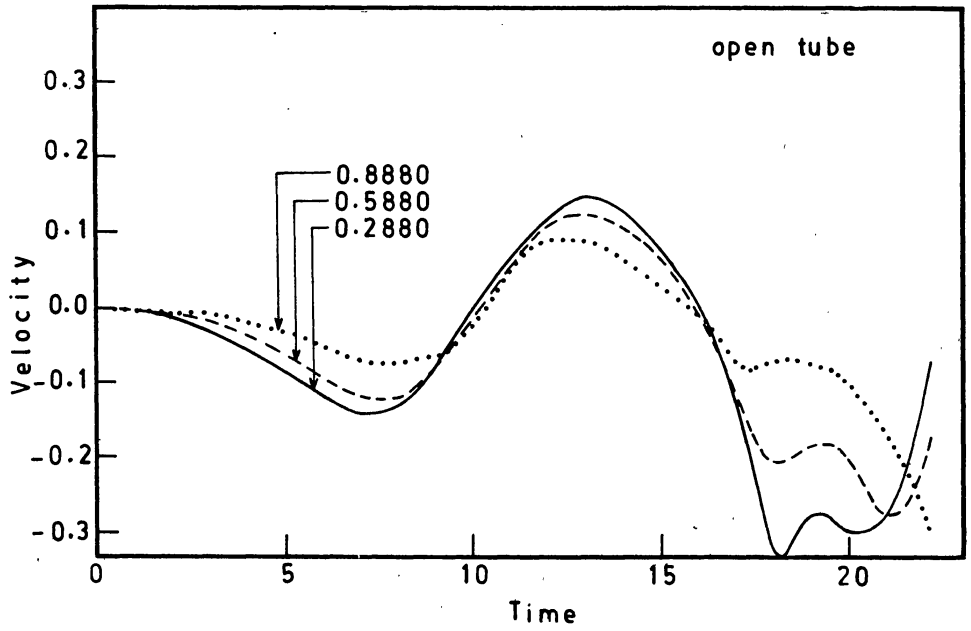

Figure 12. Response of an open tube to initial upflow is shown for $\Gamma = 3.0$, $\gamma = 1.95$ and $\beta = 6.0$. The velocity is plotted against time for $z = 0.8880$ (dotted line), 0.5880 (dashed line) and 0.2880 (solid line) respectively.

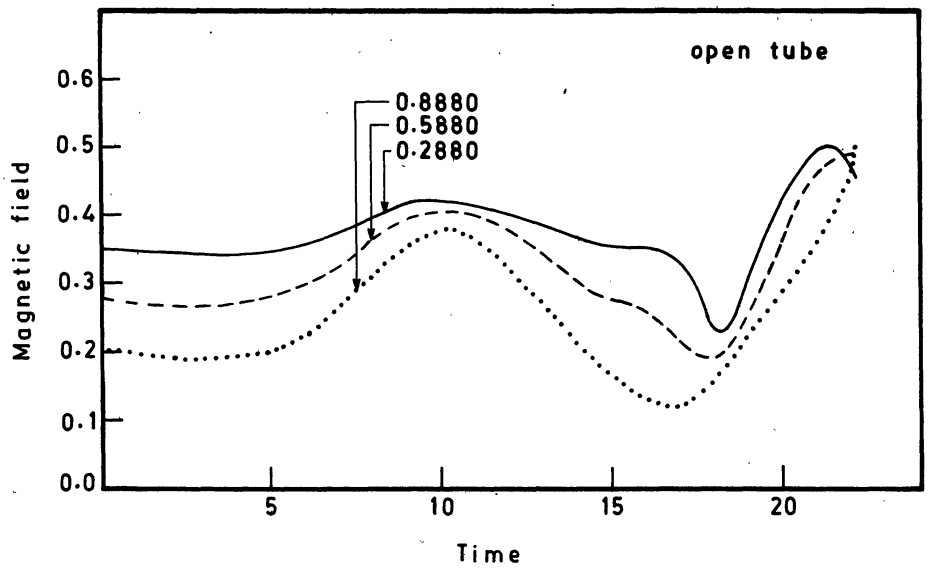

Figure 13. Magnetic field is plotted as a function of time for an open tube with $\Gamma = 3.0$, $\gamma = 1.95$, $\beta = 6.0$ at $z = 0.8880$ (dotted line), 0.5880 (dashed line) and 0.2880 (solid line) respectively.

decrease of field after the initial enhancement.

The picture changes considerably when we consider the open tube. Fig. 9 shows the linear regime for $\beta = 4.0$ and $\gamma = 1.95$. As compared to the same case for the closed tube, the changes are less rapid. Moreover, as seen in Fig. 10, the nonlinear regime shows saturation to a steady state.

Fig. 11 shows the case for $\beta = 2.0$ for an open tube. Here we see an interesting manifestation of overstability. The violent phase does not set in even after 40 free-fall time-scales. This result indicates a solution to the dilemma arising from the work of Webb & Roberts (1978). There it was seen that when the super-adiabaticity δ is $> 1/8$, the instability will occur no matter how small β is. This implies that the fluid can still be unstable even in an almost evacuated flux tube. The nonlinear calculation suggests that such an evacuated flux tube will undergo overstable oscillations. Physically it is easy to understand the overstability. When a parcel of fluid moves up due to bouyancy, it is the magnetic field gradient which acts as the additional restoring force. However, if a secular collapse of the tube takes place simultaneously, this gradient is continuously reduced (since pressure is constant at the bottom of the tube). Thus the parcel can execute greater oscillations with this decrease in the restoring force. An inspection of the phase of the oscillation at different distances from the base of the tube yields no convincing evidence for wave propagation in this case. Thus these seem to be standing waves.

Figs 12 and 13 show the result of starting with an initial updraft for $\beta = 6.0$. The flow quickly changes into a downflow and continues with attendent intensification of field until the pressure at the top of the tube vanishes (an exactly similar result is obtained for an initial downdraft as well). Thus no calculations were possible beyond this state. Such a vanishing pressure is probably a numerical artifact. Since the density is kept invariant at the boundary, the numerically induced decrease in pressure is equivalent to a decrease in temperature. It remains to be seen to what extent would inclusion of non-adiabatic processes in the energy equation prevent this numerical cooling and thus yield a physically acceptable solution. Both the velocity as well as the magnetic field show a sort of oscillatory behaviour with a period of $\sim$ 12 free-fall time-scales. Thus even in this case one does not know whether a steady state will be attained or whether the oscillatory behaviour will persist for nonadiabatic calculations. However, as compared to the closed tube, the velocities attained are much smaller.

The general picture that emerges from these results is that magnetic inhibition of convective instability does take place. When the magnetic field is very strong, the instability, if present at all, takes the form of an overstability. For smaller fields, the tube collapses to a hydrodynamic equilibrium with enhanced field. For still smaller fields the changes take place so violently that either the SFT approximation breaks down or adiabatic condition becomes unrealistic. Only two-dimensional, nonadiabatic calculations can show what the later time development would be like for very small initial magnetic fields. The details of the values demarcating these regimes of strong and weak fields depend on superadiabaticity as well as on the boundary conditions.

The answer to the question whether the final direction of flow depends on the direction of the initial perturbation in turn depends on the boundary condition applied. In the case of the closed tube, an initial upflow develops into a large upflow. However,

there seems to be no dispersal of the field taking place in this case. Instead, we see a concentration of field. Similarly it does not follow that a downflow leads unambiguously to field intensification. In the case of the open tube, both upflow and downflow lead eventually to a large downflow velocity. Since the presence of a source of mass flux is not ruled by both the boundary conditions, neither does a downflow evacuate the tube nor an upflow inundate the tube. This, perhaps, is the reason why a downflow does not lead to field intensification nor an upflow to field dispersal in an unambiguous manner.

The present study does not give a clear answer about the final dynamical status of the unstable tube. For the open tubes, a steady intense state with downflow was obtained for $\beta = 4.0$ and a tendency towards field intensification was seen for $\beta = 6.0$ albeit in an unsteady form. It was also seen that the flow at large times developed into a downflow regardless of the initial direction of the perturbation. This fact coupled with the absence of any tendency for significant field intensification with closed tubes (except for tubes with upflows) tempts one to suggest that only open tubes can attain an intense equilibrium state with downflows. This excludes the case of emerging closed tubes where downflows can occur due to changing inclination of the tube (Shibata 1980). There is also a possibility of downflows existing within weak closed tubes like the inner network fields. The earlier concept that only tubes undergoing collapse could manifest the downflow appears too restrictive in the light of the present study. We now see that downflows can continue to exist even in a fully collapsed tube. This however leads to a problem in the case of the Sun. According to the present work, convective instability leads to generation of flows given a source of mass flux. One does not know the corresponding final state in the absence of a source of gas supply. If there is no agency to decelerate the convectively induced flows in such a case of an isolated tube, then one can expect flows to continue until the tube is completely evacuated. This is indeed quite unphysical. There are two alternatives for resolving this problem. One is that there is some as yet unknown deceleration which halts the flow before the tube is completely evacuated. The observed downflows can then be interpreted as an effect of a velocity–brightness correlation in the manner suggested by Spruit (1979). A second alternative is that more gas enters the tube by some unknown way than as calculated by Giovanelli (1977). In this case the observed downflow is real and is nothing but the manifestation of convection within a slender flux tube. However, these results can only be tentatively applied to solar tubes since these span several scale-heights of varying superadiabaticity. On the other hand, since the superadiabaticity peaks only over a small height extent (Spruit 1977) and since the linear eigenfunctions of Spruit & Zweibel (1979) also peak in the same region, one does not expect the asymptotic results for a short tube to be far different from those for a tube of realistic dimensions.

4. Summary

It is seen that convective instability within slender flux tubes is inhibited by the initial magnetic field. The final state of a flux tube undergoing convective instability depends on the boundary conditions. If a constant pressure is maintained at both ends of the tube, then the final state depends on the initial perturbations as well. An initial updraft leads to a more intense tube with steady upflow. An initial downdraft does not unambiguously lead to field intensification, but develops into a large downflow. For an open tube, however, the flow develops into a downflow irrespective of initial

direction of velocity perturbation. There is also evidence for field amplification. It is thus seen that convective instability results in the generation of significant flows within slender flux tubes.

Acknowledgements

It is a pleasure to acknowledge an useful discussion with Profesor W. Unno. Helpful comments from Dr M.H.Gokhale and Dr K.R. Sivaraman are also greatly appreciated. The author has considerably benefited by earlier discussions with Dr S. S. Hasan regarding the latter's work on convective instability. The comments by Dr H. C. Spruit and an anonymous referee on an earlier version of the paper have helped in the clarification of certain important points concerning the physics of the problem.

References

Beckers, J. M., Schröter, E. H. 1968, *Solar Phys.*, **4**, 142.

Galloway, D. J., Moore, D. R. 1979, *Geophys. Astrophys. Fluid Dyn.*, **12**, 73.

Giovanelli, R. G. 1977, *Solar Phys.*, **52**, 315.

Giovanelli, R. G., Ramsay, J. V. 1971, in *IAU Symp. 43 : Solar Magnetic Fields,* Ed. R. Howard, D. Reidel, Dordrecht, p. 293.

Giovanelli, R. G., Slaughter, C. 1978, *Solar Phys.*, **57**, 255.

Harvey, J., Hall, D. 1975, *Bull. Am. astr. Soc.*, **7**, 459.

Hasan, S. S. 1982, in *IAU Symp. 102 : Solar and Stellar Magnetic Fields,* Ed. J. O. Stenflo, D. Reidel, Dordrecht.

Parker, E. N. 1963, *Astrophys. J.*, **138**, 552.

Parker, E. N. 1978, *Astrophys. J.*, **221**, 368.

Sheeley, N. R. 1971, in *IAU Symp. 43 : Solar Magnetic Fields,* Ed. R. Howard, D. Reidel, Dordrecht, p. 310.

Shibata, K 1980, *Solar Phys.*, **66**, 61.

Simon, G. W., Zirker, J. B. 1974, *Solar Phys.*, **35**, 331.

Spruit, H. C. 1977, *PhD Thesis*, University of Utrecht.

Spruit, H. C. 1979, *Solar Phys.*, **61**, 363.

Spruit, H. C., Zweibel, E. G. 1979, *Solar Phys.*, **62**, 15.

Roberts, B., Webb, A. R. 1978, *Solar Phys.*, **56**, 5.

Unno, W., Ando, H. 1979, *Geophys. Astrophys. Fluid. Dyn.*, **12**, 107.

Webb, A. R., Roberts, B. 1978, *Solar Phys.*, **59**, 249.

Webb, A. R., Roberts, B. 1980, *Solar Phys.*, **68**, 71.

Weiss, N. O. 1966, *Proc. R. Soc.*, **A293**, 310.

Zucrow, M. J., Hoffman, H. D. 1976, *Gas Dynamics*, Vol. I, John Wiley, New York.